Numerische Mathematik (2019) 142:833–862
https://doi.org/10.1007/s00211-019-01045-7

Numerische Mathematik

Error estimates for Galerkin finite element methods for the Camassa–Holm equation

D. C. Antonopoulos[1,2] · V. A. Dougalis[1,2] · D. E. Mitsotakis[3]

Received: 26 May 2018 / Revised: 25 March 2019 / Published online: 11 May 2019

Abstract
We consider the Camassa–Holm (CH) equation, a nonlinear dispersive wave equation that models one-way propagation of long waves of moderately small amplitude. We discretize in space the periodic initial-value problem for CH (written in its original and in system form), using the standard Galerkin finite element method with smooth splines on a uniform mesh, and prove optimal-order L^2-error estimates for the semidiscrete approximation. Using the fourth-order accurate, explicit, "classical" Runge–Kutta scheme for time-stepping, we construct a highly accurate, stable, fully discrete scheme that we employ in numerical experiments to approximate solutions of CH, mainly smooth travelling waves and nonsmooth solitons of the 'peakon' type.

Mathematics Subject Classification 65M60 · 35Q53

1 Introduction

In this paper we analyze standard Galerkin finite element approximations to the *Camassa–Holm* (CH) equation

$$u_t + 2ku_x + 3uu_x - u_{xxt} = 2u_x u_{xx} + uu_{xxx}. \tag{1.1}$$

✉ V. A. Dougalis
doug@math.uoa.gr

D. C. Antonopoulos
antonod@math.uoa.gr

D. E. Mitsotakis
dimitrios.mitsotakis@vuw.ac.nz

1 Mathematics Department, National and Kapodistrian University of Athens, 15784 Zographou, Greece

2 Institute of Applied and Computational Mathematics, FORTH, 70013 Heraklion, Greece

3 School of Mathematics and Statistics, Victoria University of Wellington, Wellington 6140, New Zealand

The equation may be derived as a bi-Hamiltonian integrable system by the method of [24] (cf. [22,23]). It is named after Camassa and Holm, who derived it in [7] from the Euler equations of water-wave theory as a model for the unidirectional propagation of long waves on the surface of an ideal fluid in a uniform horizontal channel. In (1.1), which is written in nondimensional, unscaled variables, $u = u(x, t)$ is proportional to the depth-averaged horizontal velocity of the fluid at x, t, that are proportional to position along the channel and time, respectively. The equation was further studied from this viewpoint in [27], and was rigorously justified in [17] as an $O(\sigma^4)$-accurate unidirectional approximation to the Euler equations when the scaling parameters satisfy $\sigma \ll 1, \varepsilon = O(\sigma)$. Here $\varepsilon = a/h_0, \sigma^2 = h_0^2/\lambda^2$, h_0 is the depth of the channel, a is a typical surface wave amplitude, and λ a typical wavelength. In scaled, nondimensional variables such a derivation leads e.g. to the equation

$$\upsilon_\tau + \upsilon_y + \varepsilon\upsilon\upsilon_y - \sigma^2\upsilon_{yy\tau} - \tfrac{\varepsilon\sigma^2}{3}(2\upsilon_y\upsilon_{yy} + \upsilon\upsilon_{yyy}) = O(\sigma^4), \tag{1.2}$$

from which we may recover (1.1) by replacing the right-hand side by zero and making the change of variables $u(x, t) = 2k\varepsilon\upsilon(y, \tau)/3$, $y = \sigma x$, $\tau = 2k\sigma t$. Hence, when compared with the scaled BBM equation, for which $\sigma \ll 1, \varepsilon = O(\sigma^2)$, the Eq. (1.2) approximates the Euler equations to the same order of formal accuracy, possesses an additional nonlinear dispersive term, and remains valid in the larger wave-amplitude regime $\varepsilon = O(\sigma)$.

The Camassa–Holm equation has been studied extensively and shown to possess global smooth solutions, but also solutions that develop 'breaking wave' singularities in finite time; in such singular solutions the derivative u_x blows up while u remains bounded. As expected from its complete integrability properties, the equation possesses solitons, i.e. solitary waves that interact cleanly. It should be noted that (1.1) may be written in system form e.g. as

$$\begin{aligned} &m = u - u_{xx}, \\ &m_t + 2ku_x + um_x + 2u_x m = 0. \end{aligned} \tag{1.3}$$

The literature on the well-posedness of the initial-value problem (ivp) for the CH is large; here we will just mention some basic references. (A survey of results up to 2003 may be found in [35]. It should be noted that in some of the works to be mentioned below k is taken equal to zero in (1.1) and in (1.3); for the significance of k in the context of travelling-wave solutions, see the remarks below.) In [15] Constantin and Escher established the existence of local in time solutions in H^3 for (1.1) with $k = 0$, and provided sufficient conditions on the initial data that lead to global solutions or to the emergence of singularities in finite time. Analogous results for the periodic ivp for the CH, written in the system form (1.3) with $k = 0$, were established in [13] in the Sobolev space H^2_{per} of periodic functions. In [33] Li and Olver studied the well-posedness of the ivp for a slightly generalized form of (1.1) in H^s for $s > 3/2$, put forth alternative conditions to those of [15] for global existence and finite-time blow up of solutions, and also studied the existence of weaker solutions in H^s for $1 < s \leq 3/2$. The development of singularities has been studied in several papers in

addition to those already mentioned, e.g. in [16,35], and in [17]; in the latter reference the large-time ($O(T/\varepsilon)$) existence of solutions and the breaking of waves of the free surface equation (in addition to the equation of the velocity u) have also been analyzed. More recently, issues of existence of global generalized solutions, possibly after wave-breaking occurs, have been studied, cf. e.g. [6]. We also note that the well-posedness of initial-boundary value problems (ibvp's) for CH (usually written in the system form (1.3)) has also been studied; see e.g. [31] for the local well-posedness in H^4 of the ibvp for (1.3) with $k = 0$ on a finite interval with boundary conditions $u = m = 0$ at the endpoints, and also [21], where the well-posedness of the quarter-plane and the two-point ibvp has been studied in more general spaces.

Since CH is completely integrable it is amenable to study in terms of the Inverse Scattering Transform (IST), cf. e.g. [12,14], and their references. A complete classification of its travelling-wave solutions has been carried out in [32]; such solutions may be smooth or nonsmooth, in the latter case satisfying the equation in the sense of distributions. Its solitary waves are solitons. If $k \neq 0$ CH possesses smooth solitons and N-solitons; these have been explicitly constructed, and their interactions studied by IST; cf. [28], and especially [36–39]. For $k = 0$ the equation does not have smooth solitary waves; it has however generalized soliton solutions ('peakons') of the form $u(x,t) = c\exp(-|x - ct|)$ for any $c > 0$; the study of existence and interactions of peakons has attracted a lot of attention, starting with [7]. (As previously mentioned, other types of singular travelling-wave solutions have been identified in [32].) Finally, let us mention that the stability of smooth solitons and peakons has been established in [19,20]; see also [18].

A note on the constant k that appears in (1.1): As the change of variables that connects the scaled version (1.2) of CH with (1.1) implies, k is related to the speed of e.g. the travelling-wave solutions of (1.2), and, therefore, for physical water waves it is necessary that $k \neq 0$. We may assume that $k > 0$, since, otherwise, the change of variables $U(X,T) = -u(x,t)$, $X = -x$, $T = t$ leads to a CH equation with $-2kU_X$ instead of $2ku_x$. It has also been noticed since [7] that the change of variables $w(z,s) = u(x,t) + k$, $z = x + kt$, $s = t$, transforms (1.1) into

$$w_s + 3ww_z - w_{zzs} = 2w_z w_{zz} + ww_{zzz}, \tag{1.4}$$

i.e. the CH without the $2ku_x$ term. (We will usually write (1.4) using the variables u, x, t and call it, cf. [36], reduced CH equation (RCH).) As a consequence of this transformation and previous remarks on the existence of solitary waves of CH and RCH, it follows that RCH possesses smooth travelling-wave solutions decaying at infinity to k, and CH with $k \neq 0$ possesses peakon-type travelling waves decaying to $-k$.

Since the derivation of CH, numerical methods have been used in an exploratory fashion to illuminate aspects of the generation and interactions of its solutions, see e.g. [8]. The ensuing numerical literature is large; we confine ourselves to mentioning a few papers that the reader may consult along with their references. Among works that focus on the analysis of numerical methods and error estimates cf. e.g. [30] (spectral methods), [11,26] (finite difference methods), and [9] (particle methods). Works that

focus on the construction of numerical schemes and numerical experimentation include e.g. [29] (spectral methods), [34,41] (DG methods), and [10] (particle methods).

In the paper at hand we consider Galerkin finite element methods for the numerical solution of CH. In Sects. 2 and 3 we provide the necessary background and notation and prove optimal-order-of-convergence L^2-error estimates for the standard Galerkin semidiscrete approximation for the periodic ivp for (1.1) using smooth splines on a uniform mesh. The proof is effected by comparing the semidiscrete approximation with the Thomée–Wendroff quasiinterpolant, [40]. In Sect. 4 we consider the analogous periodic ivp for the system (1.3) and prove L^2-error estimates of optimal rate of convergence for the semidiscrete standard Galerkin approximations of m and u using again smooth periodic splines on a uniform mesh and employing similar error estimation techniques. We refer to this numerical scheme as the 'modified' Galerkin method and note that it requires splines of order $r \geq 2$ (i.e. continuous piecewise polynomial functions of degree $r - 1 \geq 1$), thus allowing the use of piecewise linear continuous functions, as opposed to the standard Galerkin scheme for (1.1) that requires $r \geq 3$, i.e. using at least C^1 quadratics due to the presence of the uu_{xxx} term. We took $k = 0$ for simplicity in Sects. 3 and 4; the inclusion of the $2ku_x$ term poses no difficulty and the results are the same.

In Sect. 5 we present the results of some numerical experiments that we performed using the Galerkin methods described above in space and discretizing the ivp's for the attendant ode systems in the temporal variable by the classical, explicit, fourth-order-accurate Runge–Kutta scheme. The resulting fully discrete methods are stable under a mild restriction on the Courant number $\Delta t/h$, as the problem is not very stiff due to the presence of the BBM type term $-u_{xxt}$ in the left-hand side of (1.1). In the numerical experiments we check the spatial order of convergence of the schemes in the case of smooth solutions and investigate experimentally the order of convergence for peakons. We check the conservation properties of the discrete schemes and study the fidelity of the numerical approximations of the travelling waves by computing their amplitude, phase, shape, and speed errors. Finally, we study the generation and interactions of peakons and compare the accuracy of our schemes with that of other numerical methods in the literature.

In an expanded version of the paper, [1], we also consider the ibvp for the system (1.3) on a finite interval with zero Dirichlet boundary conditions for m and u at the endpoints, We study the convergence of the standard Galerkin method on a quasiuniform mesh for this problem and prove by energy methods L^2 and H^1 error estimates for its semidiscretization.

In this paper we denote, for integer $k \geq 0$, by $H^k = H^k(0,1)$ the usual L^2-based Sobolev spaces on $[0,1]$ by $\mathring{H}^1$ the subspace of H^1 consisting of functions with zero boundary conditions, and by H^k_{per} the subspace of H^k consisting of 1-periodic functions; in all cases the corresponding norms are denoted by $\|\cdot\|_k$. We let C^k denote the k-times continuously differentiable functions on $[0,1]$ and C^k_{per} the 1-periodic such functions. The inner product on $L^2 = L^2(0,1)$ is denoted by $(\cdot,\cdot)$ and the corresponding norm simply by $\|\cdot\|$. The norms of $W^k_\infty = W^k_\infty(0,1)$ and $L^\infty = L^\infty(0,1)$ are denoted by $\|\cdot\|_{k,\infty}$ and $\|\cdot\|_\infty$, respectively. For a Banach space

X, $C([0,T];X)$ denotes as usual the continuous maps from $[0,T]$ into X. $\mathbb{P}_r$ are the polynomials of degree at most r.

2 Periodic splines and the quasiinterpolant

As we will be interested in approximating solutions of the CH that are 1-periodic functions in the spatial variable, we let N be a positive integer and $h = 1/N$, $x_i = ih$, $i = 0, 1, \ldots, N$, and for integer $r \geq 2$ consider the associated N-dimensional space of smooth 1-periodic splines

$$S_h = \{\phi \in C^{r-2}_{per}[0,1] : \phi\big|_{[x_{i-1},x_i]} \in \mathbb{P}_{r-1}, 1 \leq i \leq N\}.$$

It is well known that S_h has the following approximation properties: Given a sufficiently smooth 1-periodic function υ, there exists $\chi \in S_h$ such that

$$\sum_{j=0}^{s-1} h^j \| \upsilon - \chi \|_j \leq Ch^s \| \upsilon \|_s, \quad 1 \leq s \leq r,$$

and

$$\sum_{j=0}^{s-1} h^j \| \upsilon - \chi \|_{j,\infty} \leq Ch^s \| \upsilon \|_{s,\infty}, \quad 1 \leq s \leq r,$$

for some constant C independent of h and υ. Moreover, there exists a constant C independent of h such that the inverse properties

$$\begin{aligned} \|\chi\|_\beta &\leq Ch^{-(\beta-\alpha)} \|\chi\|_\alpha, \quad 0 \leq \alpha \leq \beta \leq r-1, \\ \|\chi\|_{s,\infty} &\leq Ch^{-(s+1/2)} \|\chi\|, \quad 0 \leq s \leq r-1, \end{aligned}$$

hold for all $\chi \in S_h$. (In the sequel we shall denote by C generic constants independent of h.)

Thomée and Wendroff, [40], proved that there exists a basis $\{\phi_j\}_{j=1}^N$ of S_h with $\mathrm{supp}(\phi_j) = O(h)$, such that if υ a sufficiently smooth 1-periodic function, the associated *quasiinterpolant* $Q_h \upsilon = \sum_{j=1}^N \upsilon(x_j)\phi_j$ satisfies

$$\| Q_h \upsilon - \upsilon \| \leq Ch^r \| \upsilon^{(r)} \|. \tag{2.1}$$

In addition, they showed that the basis $\{\phi_j\}_{j=1}^N$ may be chosen so that the following properties hold:

(i) If $\psi \in S_h$, then

$$\| \psi \| \leq Ch^{-1} \max_{1 \leq i \leq N} |(\psi, \phi_i)|. \tag{2.2}$$

(It follows from (2.2) that if $\psi \in S_h$, $f \in L^2$ are such that

$$(\psi, \phi_i) = (f, \phi_i) + O(h^\alpha), \quad \text{for} \quad 1 \le i \le N,$$

then $\|\psi\| \le Ch^{\alpha-1} + \|f\|$).

(ii) Let w be a sufficiently smooth 1-periodic function and ν, κ integers such that $0 \le \nu, \kappa \le r-1$. Then

$$\left((Q_h w)^{(\nu)}, \phi_i^{(\kappa)}\right) = (-1)^\kappa h w^{(\nu+\kappa)}(x_i) + O(h^{2r+j-\nu-\kappa}), \quad 1 \le i \le N, \tag{2.3}$$

where $j = 1$ if $\nu + \kappa$ is even and $j = 2$ if $\nu + \kappa$ is odd.

(iii) Let f, g be sufficiently smooth 1-periodic functions and ν and κ as in (ii) above. Let

$$\beta_i = \left(f(Q_h g)^{(\nu)}, \phi_i^{(\kappa)}\right) - (-1)^\kappa \left(Q_h\left[(fg^{(\nu)})^{(\kappa)}\right], \phi_i\right), \quad 1 \le i \le N.$$

Then

$$\max_{1 \le i \le N} |\beta_i| = O(h^{2r+j-\nu-\kappa}), \tag{2.4}$$

where j as in (ii).

It follows from the approximation and inverse properties of S_h, and (2.1) that if $r \ge 2$, $\upsilon \in H^r_{per}(0,1) \cap W^r_\infty(0,1)$ and $V = Q_h \upsilon$, then

$$\|V - \upsilon\|_j \le Ch^{r-j}\|\upsilon\|_r, \ \ j = 0,1,2, \ \text{if } r \ge 3, \ \ j = 0,1, \ \text{if } r = 2, \tag{2.5}$$

$$\|V - \upsilon\|_{j,\infty} \le Ch^{r-j-1/2}\|\upsilon\|_{r,\infty}, \ j = 0,1,2, \ \text{if } r \ge 3, \ j = 0,1, \ \text{if } r = 2, \tag{2.6}$$

$$\|V\|_j \le C, \ \text{and } \|V\|_{j,\infty} \le C, \ \ j = 0,1,2, \ \text{if } r \ge 3, \ \ j = 0,1, \ \text{if } r = 2. \tag{2.7}$$

The inequalities (2.7) follow from (2.5) and (2.6).

3 Standard Galerkin semidiscretization of the periodic problem

In this section we consider the periodic initial-value problem for the Camassa–Holm equation in its reduced form. For $0 \le t \le T$ we seek $u = u(x,t)$, 1-periodic in x and satisfying

$$\begin{aligned} &u_t - u_{txx} + 3uu_x = 2u_x u_{xx} + uu_{xxx}, \quad 0 \le x \le 1, \quad 0 \le t \le T, \\ &u(x,0) = u_0(x), \quad 0 \le x \le 1. \end{aligned} \tag{C–H-per}$$

Constantin, [13], showed that (C–H-per) is well-posed in H^2_{per} on some temporal interval $[0, T]$, $T = T(u_0)$. Here it will be assumed that (C–H-per) has a unique solution that is sufficiently smooth for the purposes of the error estimation.

In the sequel we will denote the H^1 inner product by $A(\phi, \chi) = (\phi, \chi) + (\phi', \chi')$, $\phi, \chi \in H^1_{per}$. In addition we note that the right-hand side of the pde in (C–H-per) may be written as

$$2u_x u_{xx} + uu_{xxx} = u_x u_{xx} + (uu_{xx})_x = \tfrac{1}{2}(u_x^2)_x + (uu_{xx})_x.$$

Taking this into account and using integration by parts we define the semidiscrete approximation u_h of (C–H-per) in S_h for $r \geq 3$ as the map $u_h : [0, T] \to S_h$ such that

$$\begin{aligned}(u_{ht}, \phi) + (u_{htx}, \phi') + 3(u_h u_{hx}, \phi) + \tfrac{1}{2}(u_{hx}^2, \phi') \\ + (u_h u_{hxx}.\phi') = 0, \quad \forall \phi \in S_h, \quad 0 \leq t \leq T, \end{aligned} \tag{3.1}$$

$$u_h(0) = Q_h u_0. \tag{3.2}$$

We start the error analysis of the semidiscretization (3.1)–(3.2) by establishing its *consistency* with (C–H-per).

Lemma 3.1 *Let u, the solution of* (C–H-per)*, be sufficiently smooth and suppose that $r \geq 3$. If $U = Q_h u$ and $\psi : [0, T] \to S_h$ is such that*

$$A(\psi, \phi) = (U_t, \phi) + (U_{tx}, \phi') + 3(UU_x, \phi) + \tfrac{1}{2}(U_x^2, \phi') + (UU_{xx}, \phi'), \quad \forall \phi \in S_h, \tag{3.3}$$

then, there exists a constant C independent of h, such that

$$\max_{0 \leq t \leq T} \|\psi(t)\|_1 \leq Ch^r. \tag{3.4}$$

Proof Let $\rho = Q_h u - u = U - u$. Then

$$\begin{aligned}A(\psi, \phi) = (\rho_t, \phi) + (\rho_{tx}, \phi') + 3(UU_x - uu_x, \phi) + \tfrac{1}{2}(U_x^2 - u_x^2, \phi') \\ + (UU_{xx} - uu_{xx}, \phi'), \quad \forall \phi \in S_h. \end{aligned} \tag{3.5}$$

Since

$$\begin{aligned}UU_x - uu_x &= (\rho + u)(\rho_x + u_x) - uu_x = \rho\rho_x + u_x\rho + u\rho_x, \\ U_x^2 - u_x^2 &= \rho_x(U_x + u_x) = \rho_x(\rho_x + 2u_x) = \rho_x^2 + 2u_x\rho_x, \\ UU_{xx} - uu_{xx} &= (\rho + u)(\rho_{xx} + u_{xx}) - uu_{xx} = \rho\rho_{xx} + u_{xx}\rho + u\rho_{xx},\end{aligned}$$

we have from (3.5) that

$$\begin{aligned}A(\psi, \phi) = (\rho_t, \phi) + 3(\rho\rho_x + u_x\rho, \phi) + \tfrac{1}{2}(\rho_x^2, \phi') + (\rho\rho_{xx} \\ + u_{xx}\rho, \phi') + (\omega, \phi), \quad \forall \phi \in S_h, \end{aligned} \tag{3.6}$$

where $\omega : [0, T] \to S_h$ is defined by

$$(\omega, \phi) = (\rho_{tx}, \phi') + 3(u\rho_x, \phi) + (u_x\rho_x, \phi') + (u\rho_{xx}, \phi'), \quad \forall \phi \in S_h.$$

Note that for $1 \le i \le N$,

$$\begin{aligned}(\omega, \phi_i) &= (\rho_{tx}, \phi_i') + 3(u\rho_x, \phi_i) + (u_x\rho_x, \phi_i') + (u\rho_{xx}, \phi_i') \\ &= \big((Q_h u_t)_x - u_{tx}, \phi_i'\big) + 3\big(u(Q_h u)_x - uu_x, \phi_i\big) \\ &\quad + \big(u_x(Q_h u)_x - u_x^2, \phi_i'\big) + \big((u(Q_h u)_{xx} - uu_{xx}, \phi_i'\big).\end{aligned}$$

Therefore, from (2.4) it follows that

$$\begin{aligned}(\omega, \phi_i) = &-(Q_h u_{txx} - u_{txx}, \phi_i) + 3\big(Q_h(uu_x) - uu_x, \phi_i\big) \\ &- \big(Q_h(u_x^2)_x - (u_x^2)_x, \phi_i\big) - \big(Q_h(uu_{xx})_x - (uu_{xx})_x, \phi_i\big) + \gamma_i,\end{aligned}$$

where $\max_{1\le i\le N} |\gamma_i| \le Ch^{2r-1}$. Hence, from (2.1), (2.2) it follows that

$$\|\omega\| \le Ch^r. \tag{3.7}$$

Putting $\phi = \psi$ in (3.6) and taking into account (2.1), (2.5), and (2.6) we get

$$\|\psi\|_1^2 \le C(h^r\|\psi\| + h^{2r-3/2}\|\psi\| + h^{2r-5/2}\|\psi\|_1 + h^{2r-2}\|\psi\|_1) + \|\omega\|\|\psi\|,$$

which, by (3.7) and the fact that $r \ge 3$ yields (3.4). □

We now estimate the L^2-error of the semidiscrete scheme (3.1)–(3.2).

Proposition 3.1 *If u is the solution (assumed to be sufficiently smooth) of* (C–H-per) *in $[0, 1] \times [0, T]$, then for h sufficiently small, the semidiscrete problem* (3.1)–(3.2) *has, for $r \ge 3$, a unique solution $u_h : [0, T] \to S_h$. Moreover, there exists a constant C independent of h such that*

$$\max_{0\le t\le T} \|u(t) - u_h(t)\| \le Ch^r. \tag{3.8}$$

Proof It is clear that the ode system represented by (3.1)–(3.2) has a unique solution u_h locally in t. While the solution exists, taking $\phi = u_h$ in (3.1) and using integration by parts gives

$$\tfrac{1}{2}\tfrac{d}{dt}\big(\|u_h\|^2 + \|u_{hx}\|^2\big) + \tfrac{1}{2}(u_{hx}^2, u_{hx}) + (u_h u_{hxx}, u_{hx}) = 0.$$

Due to periodicity $(u_h u_{hxx}, u_{hx}) = \frac{1}{2}\big(u_h, \partial_x(u_{hx}^2)\big) = -\frac{1}{2}(u_{hx}, u_{hx}^2)$. Therefore, $\frac{d}{dt}\|u_h\|_1^2 = 0$, i.e. the H^1-norm of the semidiscrete solution is conserved. By standard ode theory this implies that u_h exists in any finite temporal interval.

Let now $U = Q_h u$ and $\theta = U - u_h$. From (3.5), (3.1) we have

$$A(\theta_t, \phi) + 3(UU_x - u_h u_{hx}, \phi) + \tfrac{1}{2}(U_x^2 - u_{hx}^2, \phi') + (UU_{xx} - u_h u_{hxx}, \phi') = A(\psi, \phi), \quad \forall \phi \in S_h. \tag{3.9}$$

Since

$$\begin{aligned} UU_x - u_h u_{hx} &= UU_x - (U-\theta)(U_x - \theta_x) = (U\theta)_x - \theta\theta_x, \\ U_x^2 - u_{hx}^2 &= \theta_x(U_x + u_{hx}) = \theta_x(2U_x - \theta_x) = 2U_x\theta_x - \theta_x^2, \\ UU_{xx} - u_h u_{hxx} &= UU_{xx} - (U-\theta)(U_{xx} - \theta_{xx}) = U\theta_{xx} + U_{xx}\theta - \theta\theta_{xx}, \end{aligned}$$

(3.9) implies for $\phi = \theta$ that

$$\tfrac{1}{2}\tfrac{d}{dt}\|\theta\|_1^2 + 3\big((U\theta)_x, \theta\big) + (U_x\theta_x, \theta_x) - \tfrac{1}{2}(\theta_x^2, \theta_x) + (U\theta_{xx}, \theta_x) + (U_{xx}\theta, \theta_x) - (\theta\theta_{xx}, \theta_x) = A(\psi, \theta).$$

Using again integration by parts we get

$$\tfrac{1}{2}\tfrac{d}{dt}\|\theta\|_1^2 + \tfrac{3}{2}(U_x\theta, \theta) + \tfrac{1}{2}(U_x\theta_x, \theta_x) + (U_{xx}\theta, \theta_x) = A(\psi, \theta).$$

Therefore, by (2.7) and (3.4) it follows that

$$\tfrac{d}{dt}\|\theta\|_1^2 \le C(h^{2r} + \|\theta\|_1^2), \quad t \in [0, T]. \tag{3.10}$$

Since $\theta(0) = 0$ by (3.2), Gronwall's lemma gives that $\|\theta\|_1 \le Ch^r$ on $[0, T]$; hence (3.8) follows from (2.1). □

Remark The error estimate (3.8) is still valid if $u_h(0)$ is taken as the H^1 ('elliptic') projection of u_0 on S_h, i.e. defined as $u_h(0) = \upsilon_h$, where

$$A(\upsilon_h, \phi) = A(u_0, \phi), \quad \forall \phi \in S_h. \tag{3.11}$$

Indeed, if $\varepsilon = Q_h u_0 - \upsilon_h$ we have for $\phi \in S_h$

$$A(\varepsilon, \phi) = A(Q_h u_0, \phi) - A(u_0, \phi) = (Q_h u_0 - u_0, \phi) + (\gamma, \phi), \tag{3.12}$$

where $\gamma \in S_h$ is defined for $\phi \in S_h$ by

$$(\gamma, \phi) = \big((Q_h u_0)' - u_0', \phi'\big).$$

Therefore, by (2.4) for $1 \le i \le N$,

$$(\gamma, \phi_i) = \big((Q_h u_0)' - u_0', \phi_i\big) = -(Q_h u_0'' - u_0'', \phi_i) + \beta_i,$$

where $\max_{1\le i\le N}|\beta_i| = O(h^{2r-1})$. Hence, by (2.1) and (2.2), $\|\gamma\| \le Ch^r$. It follows from (3.12) with $\phi = \varepsilon$ that $\|\varepsilon\|_1^2 \le Ch^r\|\varepsilon\|$, i.e. that $\|\varepsilon\|_1 \le Ch^r$. This implies for $\theta = U - u_h = Q_h u - u_h$, that $\|\theta(0)\|_1 = \|Q_h u_0 - \upsilon_h\|_1 \le Ch^r$ and the application of Gronwall's lemma to (3.10) gives again $\|\theta\|_1 \le Ch^r$ on $[0, T]$, i.e. that (3.8) still holds. Computing υ_h from (3.11) requires just the usual B-spline basis and not the special basis $\{\phi_i\}$. □

4 A modified Galerkin method for the periodic problem in system form

In this section we consider a *modified* Galerkin method for the periodic ivp for CH, that works also if $r = 2$, i.e. when the finite element space consists of 1-periodic, continuous, piecewise linear functions on a uniform mesh in $[0, 1]$, consequently being a subspace of H^1_{per}.

For this purpose, following [13], we write (C–H-per) in system form for two 1-periodic functions m and u as follows:

$$\begin{aligned} &m = u - u_{xx}, \\ &m_t + (mu)_x + mu_x = 0, \qquad 0 \le x \le 1, \quad 0 \le t \le T, \\ &u(x,0) = u_0(x), \quad m(x,0) = u_0(x) - u_0''(x), \quad 0 \le x \le 1. \end{aligned} \tag{C-H-s-per}$$

We will discretize (C-H-s-per) in space using approximations u_h, m_h of u, m that take values for $0 \le t \le T$ in S_h for $r \ge 2$. This will yield a *modified* Galerkin method defined for $0 \le t \le T$ by

$$(m_h, \phi) = (u_h, \phi) + (u_{hx}, \phi'), \quad \forall \phi \in S_h, \tag{4.1}$$

$$(m_{ht}, \phi) + \big((m_h u_h)_x, \phi\big) + (m_h u_{hx}, \phi) = 0, \quad \forall \phi \in S_h, \tag{4.2}$$

with initial value

$$(m_h(0), \phi) = (u_0, \phi) + (u_0', \phi'), \quad \phi \in S_h, \tag{4.3}$$

i.e. with $m_h(x, 0)$ taken as the L^2-projection of $m(x, 0)$ on S_h. Compatibility with (4.1) and (4.3) imply that $u_h(0)$ satisfies for $\phi \in S_h$

$$A(u_h(0), \phi) = A(u_0, \phi), \tag{4.4}$$

i.e. that $u_h(0)$ is the H^1 projection of u_0 in S_h. We first establish the *consistency* of (4.1)–(4.3) with (C-H-s-per).

Lemma 4.1 *Let (m, u), the solution of* (C-H-s-per) *in $[0, 1] \times [0, T]$, be sufficiently smooth and suppose that $r \ge 2$. If $M = Q_h m$, $U = Q_h u$ and $\psi, \zeta : [0.T] \to S_h$ are such that*

$$\begin{aligned}&(U,\phi)+(U_x,\phi')-(M,\phi)=(\psi,\phi),\quad \forall\phi\in S_h,\\&(M_t,\phi)+\big((MU)_x,\phi\big)+(MU_x,\phi)=(\zeta,\phi)\quad \forall\phi\in S_h,\end{aligned}\tag{4.5}$$

then, there exists a constant C independent of h, such that

$$\max_{0\le t\le T}(\|\psi(t)\|+\|\zeta(t)\|)\le Ch^r.\tag{4.6}$$

Proof Let $\rho=Q_hu-u=U-u$, and $\sigma=Q_hm-m=M-m$. Then

$$\begin{aligned}&(\psi,\phi)=(\rho,\phi)+(\rho_x,\phi')-(\sigma,\phi)=(\rho-\sigma,\phi)+(\widetilde{\psi},\phi),\quad \forall\phi\in S_h,\\&(\zeta,\phi)=(\sigma_t,\phi)+\big((MU)_x-(mu)_x,\phi\big)+(MU_x-mu_x,\phi),\quad \forall\phi\in S_h,\end{aligned}\tag{4.7}$$

where $\widetilde{\psi}:[0,T]\to S_h$ satisfies

$$(\widetilde{\psi},\phi)=(\rho_x,\phi'),\quad \forall\phi\in S_h.\tag{4.8}$$

Since

$$\begin{aligned}&MU-mu=(m+\sigma)(u+\rho)-mu=m\rho+u\sigma+\sigma\rho,\\&MU_x-mu_x=(m+\sigma)(u_x+\rho_x)-mu_x=m\rho_x+u_x\sigma+\sigma\rho_x,\end{aligned}$$

it follows from the second equation of (4.7) that

$$\begin{aligned}(\zeta,\phi)=&(\sigma_t,\phi)+(m_x\rho,\phi)+2(u_x\sigma,\phi)+(\sigma_x\rho,\phi)+2(\sigma\rho_x,\phi)\\&+(\widetilde{\zeta},\phi),\quad \forall\phi\in S_h,\end{aligned}\tag{4.9}$$

where $\widetilde{\zeta}:[0,T]\to S_h$ is defined as

$$(\widetilde{\zeta},\phi)=2(m\rho_x,\phi)+(u\sigma_x,\phi),\quad \forall\phi\in S_h.\tag{4.10}$$

It follows from (4.8) for $1\le i\le N$,

$$(\widetilde{\psi},\phi_i)=(\rho_x,\phi_i')=\big((Q_hu)_x,\phi_i'\big)-(u_x,\phi_i')=-(Q_hu_{xx}-u_{xx},\phi_i)+\gamma_i,$$

where, from (2.4), $\max_{1\le i\le N}|\gamma_i|\le Ch^{2r-1}$. Therefore, from (2.1) and (2.2) we see that

$$\|\widetilde{\psi}\|\le Ch^r.\tag{4.11}$$

Putting $\phi=\psi$ in the first equation of (4.7) and taking into account (2.1) and (4.11) we get

$$\|\psi\|\le Ch^r.\tag{4.12}$$

In addition, from (4.10) it follows for $1 \le i \le N$

$$\begin{aligned}(\widetilde{\zeta}, \phi_i) &= 2\big(m(Q_h u)_x, \phi_i\big) - 2(mu_x, \phi_i) + \big(u(Q_h m)_x, \phi_i\big) - (um_x, \phi_i)\\ &= 2\big(Q_h(mu_x) - mu_x, \phi_i\big) + \big(Q_h(um_x) - um_x, \phi_i\big) + \widetilde{\gamma}_i,\end{aligned}$$

where, by (2.4), $\max_{1\le i\le N} |\widetilde{\gamma}_i| \le Ch^{2r+1}$. Consequently, from (2.1) and (2.2) we have

$$\|\widetilde{\zeta}\| \le Ch^r. \tag{4.13}$$

Finally, if we take $\phi = \zeta$ in (4.9), we obtain, in view of (4.13),

$$\|\zeta\| \le Ch^r,$$

which, together with (4.12), establishes (4.6). □

We proceed now to derive an L^2-error estimate for the solution of the semidiscrete problem (4.1)–(4.3).

Proposition 4.1 *If the solution (m, u) of (C-H-s-per) on $[0, 1] \times [0, T]$ is sufficiently smooth, then, for h sufficiently small, the semidiscrete problem (4.1)–(4.3) has, for $r \ge 2$, a unique solution on $[0, T]$ that satisfies*

$$\max_{0\le t\le T} (\|m(t) - m_h(t)\| + \|u(t) - u_h(t)\|) \le Ch^r. \tag{4.14}$$

Proof For every $t \ge 0$ we may solve the linear discrete problem (4.1) and express u_h in terms of m_h. Upon substituting u_h in (4.2), we easily see that the resulting initial-value problem (4.2)–(4.3) has a unique solution m_h locally in t. While this solution exists, putting $M = Q_h m$, $U = Q_h u$, $\theta = U - u_h$, and $\xi = M - m_h$, from (4.1), (4.2), (4.5) we obtain

$$\begin{aligned}&(\theta, \phi) + (\theta_x, \phi') - (\xi, \phi) = (\psi, \phi), \quad \forall \phi \in S_h,\\ &(\xi_t, \phi) + \big((MU - m_h u_h)_x, \phi\big) + (MU_x - m_h u_{hx}, \phi) = (\zeta, \phi), \quad \forall \phi \in S_h.\end{aligned} \tag{4.15}$$

With $\phi = \theta$ in the first equation above we see, in view of (4.6), that

$$\|\theta\|_1 \le \|\xi\| + Ch^r. \tag{4.16}$$

Now

$$\begin{aligned}MU - m_h u_h &= MU - (M - \xi)(U - \theta) = M\theta + U\xi - \theta\xi,\\ MU_x - m_h u_{hx} &= MU_x - (M - \xi)(U_x - \theta_x) = M\theta_x + U_x\xi - \theta_x\xi.\end{aligned}$$

Hence, from the second equation in (4.15), putting $\phi = \xi$ we obtain

$$\tfrac{1}{2}\tfrac{d}{dt}\|\xi\|^2 + \big((M\theta)_x, \xi\big) + \big((U\xi)_x, \xi\big) - \big((\theta\xi)_x, \xi\big) + (M\theta_x, \xi) + (U_x\xi, \xi) - (\theta_x\xi, \xi) = (\zeta, \xi).$$

Using integration by parts we see that $\big((U\xi)_x, \xi\big) = -(U\xi, \xi_x) = \frac{1}{2}(U_x\xi, \xi)$, and similarly, $\big((\theta\xi)_x, \xi\big) = \frac{1}{2}(\theta_x\xi, \xi)$. Therefore, we may write the above equation as

$$\tfrac{1}{2}\tfrac{d}{dt}\|\xi\|^2 + (M_x\theta, \xi) + 2(M\theta_x, \xi) + \tfrac{3}{2}(U_x\xi, \xi) - \tfrac{3}{2}(\theta_x\xi, \xi) = (\zeta, \xi).$$

Consequently, from (2.7), (4.6), (4.16), we get for some constant C independent of h, that

$$\tfrac{d}{dt}\|\xi\|^2 \le C(\|\xi\|^2 + h^r\|\xi\|) + 3|(\theta_x\xi, \xi)|. \tag{4.17}$$

The definition of $m_h(0)$ by (4.3) implies that for $\xi(0) = Q_h m(0) - m_h(0)$ we have if $1 \le i \le N$

$$\begin{aligned}\big(\xi(0), \phi_i\big) &= \big(Q_h m(0) - m_h(0), \phi_i\big) = \big(Q_h(u_0 - u_0''), \phi_i\big) - (u_0, \phi_i) - (u_0', \phi_i') \\ &= (Q_h u_0 - u_0, \phi_i) - (Q_h u_0'' - u_0'', \phi_i).\end{aligned}$$

Therefore, by (2.2) and (2.1) we conclude that

$$\|\xi(0)\| \le Ch^r, \tag{4.18}$$

from which, by inverse properties, we see that $\|\xi(0)\|_\infty = O(h^{r-1/2})$. By continuity we may infer that there is a maximal time $t_h \in (0, T]$ such that the solution of (4.1)–(4.3) exists for $0 \le t \le t_h$ and satisfies

$$\max_{0\le t\le t_h} \|\xi(t)\|_\infty \le 1. \tag{4.19}$$

Therefore, from (4.17) it follows that

$$\tfrac{d}{dt}\|\xi\|^2 \le C(\|\xi\|^2 + h^r\|\xi\|) + 3\|\theta\|_1\|\xi\| \le C(h^{2r} + \|\xi\|^2),$$

for $t \le t_h$. From this inequality and Gronwall's lemma we infer that

$$\|\xi(t)\| \le C_T(\|\xi(0)\| + h^r),$$

for $t \le t_h$. Hence, by (4.18)

$$\|\xi(t)\| \le C_T h^r, \quad 0 \le t \le t_h, \tag{4.20}$$

from which, by inverse properties we conclude that

$$\|\xi(t)\|_\infty \le C_T h^{r-1/2},$$

for $t \leq t_h$. Therefore, if h is taken sufficiently small, t_h is not maximal and one can consequently take $t_h = T$. Hence, (4.20) holds for $t \in [0, T]$. By (4.16), $\|\theta\|_1 \leq Ch^r$ on $[0, T]$ and (4.14) follows in view of (2.1). □

5 Numerical experiments

In this section we present the results of some numerical experiments that we performed to approximate solutions of the Camassa–Holm equation, in its reduced form RCH (i.e. with $k = 0$ in (1.1)). using the Galerkin finite element methods analyzed in the previous sections to discretize the equation in the spatial variable. In various places in the sequel use will be made of formulas of exact smooth travelling-wave solutions of RCH in the notation of [37] (see specifically formulas (2.29)–(2.30) in that reference): Let $\kappa > 0$, $p > 0$, be two parameters such that $0 < \kappa p < 1$, and $\tilde{c} = 2\kappa^2/(1-\kappa^2 p^2)$, $V = \tilde{c} + \kappa^2$. Then for $x_0 \in \mathbb{R}$ the formulas

$$u(\xi) = \kappa^2 + \frac{\tilde{c}^2 p^2 \operatorname{sech}^2 \frac{1}{2}\theta}{2 + \tilde{c} p^2 \operatorname{sech}^2 \frac{1}{2}\theta}, \tag{5.1}$$

with

$$\xi = x - Vt + x_0 = \frac{\theta}{\kappa p} + \ln\left[\frac{(1+\kappa p) + (1-\kappa p)e^{\theta}}{(1-\kappa p) + (1+\kappa p)e^{\theta}}\right], \tag{5.2}$$

define parametrically a family of single-pulse travelling-wave solutions of (RCH) that are centered at $x = x_0$, travel to the right with speed V and decay exponentially as $|x| \to \infty$ to κ^2. (As a consequence of the change-of-variable formula that transforms (1.1) into the RCH (1.4), it is seen that (1.1) with $k = \kappa^2$ possesses smooth solitary-wave solutions decaying to zero as $|x| \to \infty$, and found by replacing u in (5.1) by $u + \kappa^2$ and putting $V = \tilde{c}$.) As $\kappa \to 0$ with $\kappa p \to 1$, the solution (5.1)–(5.2) of the RCH tends to the one-parameter family of peakon (soliton) solutions of the RCH given explicitly by

$$u(x, t) = \tilde{c} \exp\left(-|x - \tilde{c}t + x_0|\right). \tag{5.3}$$

(The corresponding non-smooth travelling wave solutions of CH with $k \neq 0$ are given by $u = \tilde{u} - k$, where $\tilde{u} = \tilde{c} \exp\left(-|x - (\tilde{c} - k)t + x_0|\right)$. In the numerical experiments we compute numerically the solution (5.1)–(5.2) for each (x, t), given the parameters κ, p, by solving (5.2) for θ by Newton's method with absolute error tolerance 10^{-10} and substituting in (5.1).

5.1 Fully discrete schemes and stability conditions

We used the classical, explicit, four-stage, fourth-order accurate Runge–Kutta scheme with a uniform time step (RK4) for the temporal discretization of the o.d.e. systems

Table 1 Maximum Courant number $V\Delta t/h$ for stability for various spatial discretizations

	Standard Galerkin		Modified Galerkin		
	Cubic	Quadratic	Cubic	Quadratic	Linear
Travelling wave $V = 4$	2.92	3.91	2.62	2.93	3.93
Travelling wave $V = 6$	2.18	2.68	1.98	2.18	1.79
Peakons	1.54	1.83	1.41	1.54	1.83

representing the various space-discrete finite element schemes of the previous sections. (Unless otherwise mentioned, we solved numerically the periodic initial-value problem for RCH.) The integrals in the finite element equations were approximated by Gauss–Legendre quadrature with five nodes in each mesh interval for cubic and quadratic splines and with three nodes for piecewise linear discretizations. The initial conditions of the fully discrete scheme were normally taken as the 'elliptic' (H^1) projections of the initial data; taking the L^2 projections gave practically the same results.

Due to the presence of the $-u_{xxt}$ term in the left-hand side of RCH the o.d.e. semidiscrete systems are only mildly stiff and the fully discrete schemes were stable under a Courant number restriction. To get some indication of the maximum allowed Courant number we approximated two smooth travelling wave solutions given by (5.1)–(5.2) corresponding to $\kappa = 1$ and $V = 4$, and $V = 6$, on $[-100, 100]$ with $h = 0.1$, and tested the stability of the code integrating up to $T = 100$. We also studied the stability of the code for peakons given by (5.3) for $V = \tilde{c} = 1, 2, 3$ on $[-100, 100]$ with $h = 0.05$. The maximum allowed values of the Courant number $V\Delta t/h$ for stability are recorded in Table 1. They depend on V in the case of smooth travelling waves but are independent of V for peakons.

5.2 Spatial convergence rates

We performed a series of numerical experiments with our fully discrete schemes in order to compute the numerical rates of convergence of the spatial discretizations in various norms. (In all cases we checked that the errors practically did not change when we computed with smaller values of Δt. Usually we took $\Delta t/h = 1/10$.)

In the case of smooth solutions of the periodic ivp the numerical experiments confirm the theoretical $O(h^r)$ L^2-error convergence rates. (We experimented, on uniform meshes, with cubic and quadratic splines for the standard Galerkin method, and with cubic, quadratic, and linear splines for the modified scheme). The numerical values of the convergence rates in other norms were practically equal those expected from the approximation properties of the finite element spaces, namely $r - 1$ for the H^1 norm in all cases, r for the L^∞ norm in all cases, and $r - 2$ in the case of the H^2 norm for cubic and quadratic splines. It is noteworthy that for the same test problem the values of the two spatial discretizations (standard and modified) were very close in all norms.

In order to find the numerical convergence rates in the case of nonsmooth solutions we computed the evolution of the peakon of unit speed $u(x, t) = \exp(-|x - t|)$ on the interval $[-40, 40]$ with periodic boundary conditions, up to $T = 1$, using uniform

meshes in space with $h = 80/N$ and $\Delta t/h = 1/10$, $\Delta t = 1/M$. We used cubic, quadratic, and linear splines. Table 2 shows the observed errors (normalized by the corresponding norm of the exact solution at $T = 1$) and convergence rates in the L^2 and H^1 norms in the case of cubic splines at $T = 1$.

The experimental rates of the L^2 errors are equal to about 1.1 for both Galerkin methods and those of the H^1 errors between 0.4 and 0.5. The errors of the modified method are slightly smaller. In Table 3 we compare the normalized L^2, L^∞, and H^1 errors and convergence rates of the cubic ($r = 4$), quadratics ($r = 3$), and linear ($r = 2$) spline discretizations for the same test problem. We show only the data for the line corresponding to $N = 5120$, $M = 640$). As expected from the low regularity of the solution, the rates of convergence for all spline discretizations were roughly the same for a given norm. It appears that the modified scheme with cubic splines yields the smallest errors.

5.3 Conservation of invariants

It is well known, cf. [7], and easy to check, that solutions of the Cauchy problem of the CH Eq. (1.1) and also of the periodic ivp for (1.1) on an interval (a, b) satisfy the conservation laws $\frac{d}{dt} H_i[u] = 0$, $i = 0, 1, 2$, where

$$H_0[u] = \int_a^b u \, dx, \quad H_1[u] = \int_a^b (u^2 + u_x^2) \, dx,$$
$$H_2[u] = \int_a^b u(u^2 + u_x^2 + 2ku) \, dx. \tag{5.4}$$

In the case of the periodic ivp for the CH in the system form (1.3) it holds that $\frac{d}{dt} \tilde{H}_i[m, u] = 0$, $i = 0, 1, 2$, where

$$\tilde{H}_0[m, u] = \int_a^b m \, dx, \quad \tilde{H}_1[m, u] = \int_a^b mu \, dx,$$
$$\tilde{H}_2[m, u] = \int_a^b (u^2 m - u u_x^2 + 2ku^2) \, dx. \tag{5.5}$$

In order to assess the quality of the numerical approximations, it is important to check the extent to which the fully discrete schemes under study preserve these invariants. (As usual, we consider the RCH equation). The standard Galerkin semidiscretization (3.1) clearly preserves H_0 and H_1 in the sense that $H_i[u_h(t)] = H_i[u_h(0)]$, $i = 0, 1$. The invariant H_0 is also trivially preserved by the full discretization of (3.1) by the RK4 scheme, in contrast to H_1 which is not preserved. The modified Galerkin method (4.1)–(4.2) for the periodic ivp preserves $\tilde{H}_1$: Let m_h, u_h be the solution of (4.1)–(4.4). Then, using (4.2) with $\phi = u_h$, and (4.1) with $\phi = u_{ht}$ we have

Table 2 L^2 and H^1 normalized errors and convergence rates at $T = 1$, peakon solution, cubic splines, $h = 80/N$, $\Delta t = 1/M$

N	M	Standard Galerkin				Modified Galerkin			
		L^2 error	Rate	H^1 error	Rate	L^2 error	Rate	H^1 error	Rate
160	20	1.1109×10^{-1}	–	4.1633×10^{-1}	–	1.0346×10^{-1}	–	4.0152×10^{-1}	–
320	40	5.1323×10^{-2}	1.114	3.1138×10^{-1}	0.419	4.6734×10^{-2}	1.147	2.9610×10^{-1}	0.439
640	80	2.3124×10^{-2}	1.150	2.3106×10^{-1}	0.430	2.0617×10^{-2}	1.181	2.1716×10^{-1}	0.447
1280	160	1.0417×10^{-2}	1.150	1.7091×10^{-1}	0.435	9.1382×10^{-3}	1.174	1.5881×10^{-1}	0.451
2560	320	4.7544×10^{-3}	1.132	1.2626×10^{-1}	0.437	4.1283×10^{-3}	1.146	1.1600×10^{-1}	0.453
5120	640	2.2090×10^{-3}	1.106	9.3242×10^{-2}	0.437	1.9097×10^{-3}	1.112	8.4706×10^{-2}	0.454

Table 3 L^2, L^∞, and H^1 normalized errors and convergence rates at $T = 1$, peakon solutions, splines of order r, $N = 80/h = 5120$, $M = 1/\Delta t = 640$

Norm	Standard Galerkin		Modified Galerkin		
	$r = 4$	$r = 3$	$r = 4$	$r = 3$	$r = 2$
L^2 error	2.2090×10^{-3}	3.3557×10^{-3}	1.9097×10^{-3}	2.6936×10^{-3}	3.3828×10^{-3}
Rate	1.106	1.064	1.112	1.060	1.125
L^∞ error	7.2834×10^{-3}	1.1634×10^{-2}	6.5729×10^{-3}	7.9459×10^{-3}	1.3519×10^{-2}
Rate	0.902	0.798	0.941	0.848	0.814
H^1 error	9.3241×10^{-2}	1.0899×10^{-1}	8.4706×10^{-2}	9.0104×10^{-2}	1.1564×10^{-1}
Rate	0.437	0.403	0.454	0.443	0.407

$$\begin{aligned}\frac{d}{dt}\tilde{H}_1[m_h, u_h] &= (m_{ht}, u_h) + (m_h, u_{ht}) \\ &= -((m_h u_h)_x, u_h) - (m_h u_{hx}, u_h) + (u_h, u_{ht}) + (u_{hx}, u_{hxt}) \\ &= \frac{1}{2}\frac{d}{dt}\|u_h\|_1^2.\end{aligned}$$

On the other hand (4.1) with $\phi = u_h$ gives $(m_h, u_h) = \|u_h\|_1^2$, i.e. $\frac{d}{dt}\tilde{H}_1[m_h, u_h] = \frac{d}{dt}\|u_h\|_1^2$. From these identities we conclude that $\frac{d}{dt}\tilde{H}_1[m_h, u_h] = \frac{d}{dt}\|u_h\|_1^2 = 0$, as claimed. Note that the temporal discretization of (4.1)–(4.4) with RK4 does not conserve $\tilde{H}_1$.

In what follows we present some graphs of the temporal evolution of the invariants using the fully discrete schemes. We computed the quantities

$$E_i(t) = \log_{10}\left|\frac{H_i(t) - H_i(0)}{H_i(t)}\right|,$$

(and the analogous $\tilde{H}_i$ in the case of the modified method) for $t \geq \Delta t$. Here, $H_i(t) = H_i\left(u_h(t)\right)$ and $\tilde{H}_i(t) = \tilde{H}_i\left[m_h(t), u_h(t)\right]$. In the case of the *smooth solutions* we solved numerically the periodic ivp for the RCH on the spatial interval $[-50, 50]$ up to $t = 100$ with the standard and modified method using as initial condition $u_0(x) = 1 + e^{-x^2}$.

Figure 1 shows the graphs of the logarithmic relative errors E_i of H_i as functions of t for this example, produced for $h = 0.1$ and diminishing $\Delta t/h$ by the standard Galerkin method with cubic splines coupled with RK4 time stepping. H_0 is preserved to roundoff as expected, while H_2 is preserved to about 8 decimal digits for this value of h. (The error in H_2 is practically due to the spatial approximation since it remains almost constant as Δt is decreased.) The error in H_1 also diminishes with Δt; for $\frac{\Delta t}{h} = \frac{1}{200}$ its temporal discretization part is practically negligible and H_1 is preserved to roundoff as expected.

In the case of the modified Galerkin fully discrete scheme the cubic spline results for the preservation of the $H_i = H_i[u_h]$ are practically the same with those shown in

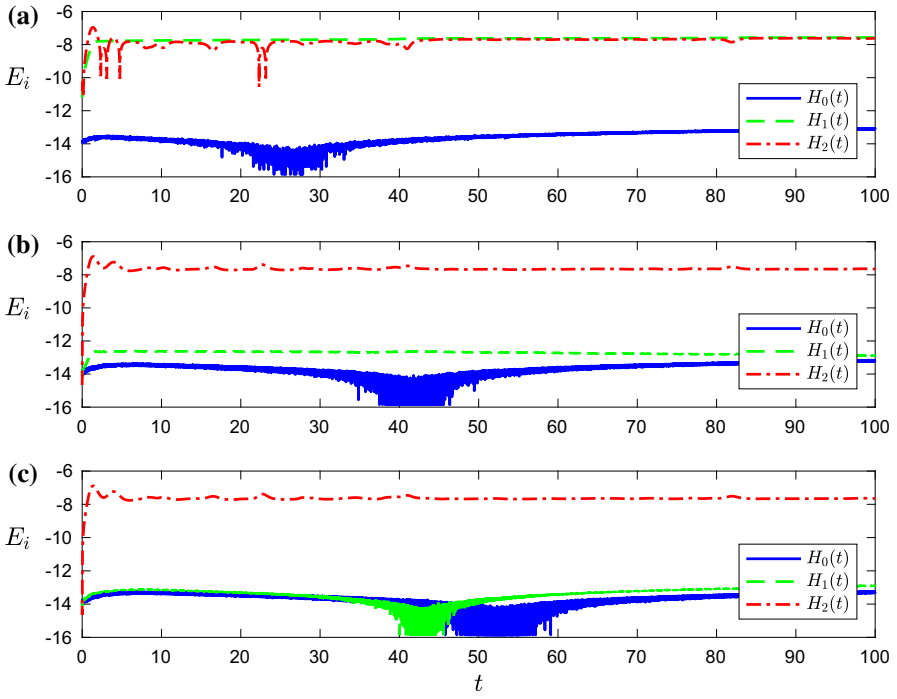

Fig. 1 Preservation of invariants H_0, H_1, H_2, smooth solutions. Standard Galerkin method with cubic splines, $h = 0.1$, **a** $\frac{\Delta t}{h} = \frac{1}{10}$, **b** $\frac{\Delta t}{h} = \frac{1}{100}$, **c** $\frac{\Delta t}{h} = \frac{1}{200}$

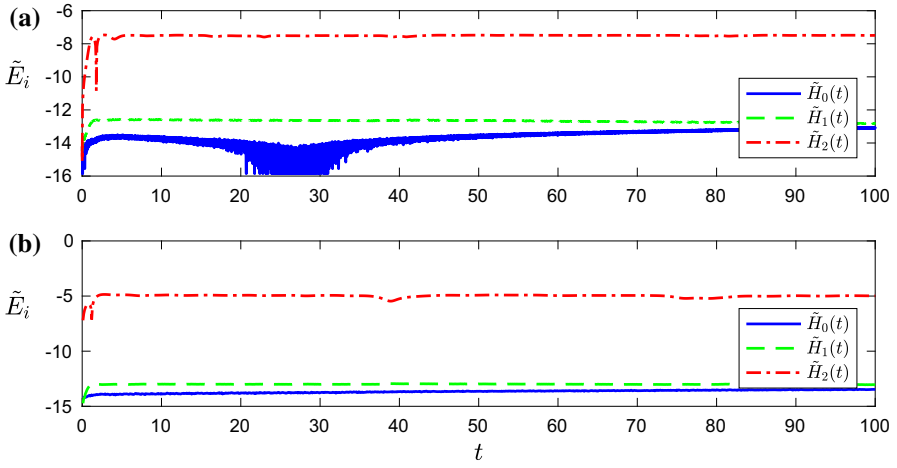

Fig. 2 Preservation of invariants $\tilde{H}_0$, $\tilde{H}_1$, $\tilde{H}_2$, smooth solutions. modified Galerkin method, $h = 0.1$, $\Delta t = 10^{-3}$, **a** cubic splines, **b** p.w. linear continuous functions

Fig. 1. In Fig. 2 we show the evolution of the logarithmic errors $\tilde{E}_i$ of the invariants $\tilde{H}_i[m_h, u_h]$ pertinent to the system form of RCH for the fully discrete schemes with cubic splines and piecewise linear functions (the latter are admitted by the modified

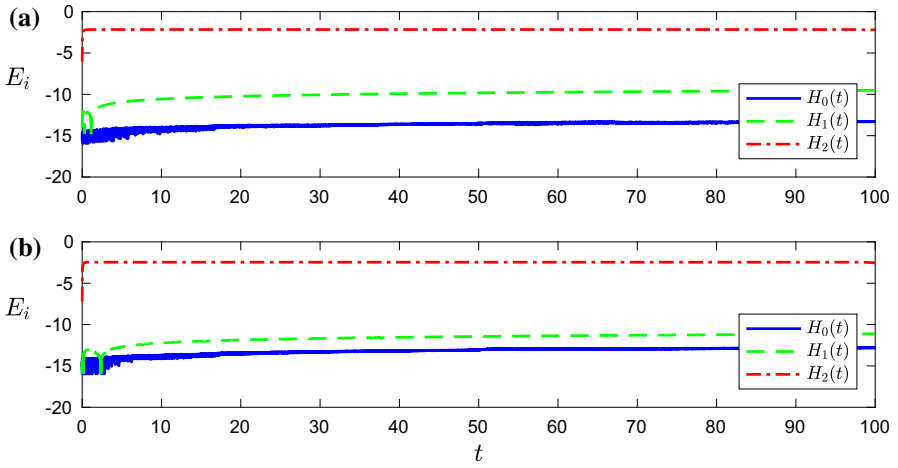

Fig. 3 Preservation of invariants H_0, H_1, H_2, peakon, $A = 1$. Standard Galerkin method with cubic splines, **a** $h = 0.1$, $\Delta t = 10^{-3}$, **b** $h = 0.05$, $\Delta t = 2.5 \times 10^{-4}$

scheme), for the same example, with $h = 0.1$ and $\Delta t = 10^{-3}$. For cubic splines $\tilde{H}_2$ is preserved to at least 7 decimal digits and to about 5 digits for the less accurate discretization with piecewise linear functions. For both discretizations the relative error of $\tilde{H}_1$ is of $O(10^{-13})$ and is due to the temporal discretization as $\tilde{H}_1$ is preserved for both semidiscrete schemes. Apparently $\tilde{H}_0$ seems to be preserved to almost roundoff in both cases. In the case of *peakons* we computed the logarithmic errors of the invariants as functions of t in several test runs. In Fig. 3, as an example, we show the results in the case of a peakon of unit amplitude and speed approximated by the standard Galerkin method with cubic splines for our usual (a), and a finer mesh (b). We observe that H_0 is preserved to roundoff, that the error of H_1 is small and is reduced by at most two digits in (b), while that of H_2 practically remains the same. This is due of course to the lack of smoothness of the solution that reduces the rate of convergence of the schemes, cf. Sect. 5.2.

5.4 Error indicators for travelling waves

In order to further assess the accuracy of our numerical methods we studied several error indicators pertinent to travelling-wave solutions, namely the *amplitude*, *phase*, *speed*, and *shape* errors, [4,5], for smooth travelling waves and peakons. Since the amplitude of the travelling wave remains constant, we define the (normalized) *amplitude error* at $t = t^n = n\,\Delta t$ as

$$E_{amp}(t^n) = \frac{|U(x^*(t^n), t^n) - U_0|}{|U_0|}, \tag{5.6}$$

where $U(x, t^n)$ is the fully discrete numerical approximation at t^n, U_0 is the initial amplitude (peak value) of the exact travelling wave and $x^*(t^n)$ is the point where $U(\cdot, t^n)$ achieves its maximum. The value of $x^*(t^n)$ is found by solving the equation

$\frac{d}{dx}U(x,t^n)=0$ by Newton's method (with tolerance 10^{-10}) for smooth solutions and by the bisection method for peakons. (For piecewise linear functions we took as x^* the mesh point where $max_i U(x_i,t^n)$ occurs.) As initial value for the Newton iteration we took the quadrature node at which U has a discrete maximum. We started the bisection method by taking an interval of length $4h$ around that quadrature node.

Finding $x^*(t^n)$ enables us to compute a *phase error* of the numerical solution U at t^n as

$$E_{phase}(t^n)=|x^*(t^n)-Vt^n|, \tag{5.7}$$

for a travelling wave of speed V, initially centered at $x=0$, and a *speed error* defined as

$$E_{speed}(t^n)=|V-V_h(t^n,\tau)|, \tag{5.8}$$

where $V_h(t^n,\tau)=(x^*(t^n)-x^*(t^n-\tau))/\tau$. We usually take τ much larger than Δt to smooth out oscillations in the discrete speed $V_h(t^n,\tau)$. (In the computations to be reported in the sequel on the temporal interval $[0,100]$, we normally take $\tau=1$.)

Finally, the (normalized) *shape error* measures the amount by which the numerical solution at t^n differs from the exact travelling wave profile $u(\cdot,t^n)$ traslated so as to give the best fit. It is defined with respect to the L^2 norm as

$$E_{shape}(t^n)=\min_s \zeta(s), \quad \zeta(s):=\frac{\|U(\cdot,t^n)-u(\cdot,s)\|}{\|u(\cdot,0)\|}, \tag{5.9}$$

where the minimum of $\zeta(s)$ is found again using the Newton or the bisection method to solve $\frac{d}{ds}\zeta^2(s)=0$ in the vicinity of t^n.

In Table 4 we show the values of the amplitude, phase and shape error at $t^n=100$ of the fully discrete approximations produced by the standard and the modified Galerkin method in the case of a smooth travelling wave of the form (5.1)–(5.2) with $\kappa=1$ and $V=4.333$. We took the spatial interval $[-100,100]$ and computed with $h=0.1$, 0.05, 0.025 and $\Delta t=h/10$.

As expected, cubic splines ($r=4$) give the best results, while there is not much difference between the standard and the modified methods for $r=4$ and $r=3$. Over time, all these errors oscillate somewhat about mean values that remain practically constant in t for $h=0.05$ and $h=0.025$.

The speed errors were practically the same for both Galerkin methods with cubic and quadratic splines for the same value of h and diminished of course with h. The number of conserved digits of the speed was equal to five for $h=0.1$, six for $h=0.05$ and seven for $h=0.025$. In the case of piecewise linear functions with the modified method the numerical speed preserved one correct digit for $h=0.1$ and two for $h=0.05$ and $h=0.025$.

In Table 5 we show the analogous errors produced by the numerical approximations with the modified method of a peakon of speed $V=1.333$. We took $h=0.05$, 0.025 and 0.01 on the interval $[-100,100]$ with $\Delta t=h/10$ and show the errors at $t^n=100$.

Table 4 E_{amp}, E_{phase}, E_{shape} at $T = 100$, mean value over the temporal interval [80, 100] for linear splines E_{phase} (a) standard Galerkin, (b) modified Galerkin, smooth travelling wave, $\kappa = 1$, $V = 4.333$

h	$r = 4$, cubic splines			$r = 3$, quadratic splines		
	E_{amp}	E_{phase}	E_{shape}	E_{amp}	E_{phase}	E_{shape}
(a) Standard Galerkin						
0.1	9.1617×10^{-9}	7.0771×10^{-6}	1.2058×10^{-8}	5.4368×10^{-7}	2.6859×10^{-5}	1.0699×10^{-7}
0.05	5.5416×10^{-10}	3.1641×10^{-7}	5.6834×10^{-10}	3.2712×10^{-8}	1.5455×10^{-6}	6.6264×10^{-9}
0.025	6.7388×10^{-11}	1.6421×10^{-8}	3.5359×10^{-11}	2.0090×10^{-9}	9.0883×10^{-8}	4.1343×10^{-10}
h	$r = 4$, cubic splines			$r = 3$, quadratic splines		
	E_{amp}	E_{phase}	E_{shape}	E_{amp}	E_{phase}	E_{shape}
(b) Modified Galerkin						
0.1	8.6377×10^{-9}	7.0627×10^{-6}	1.2004×10^{-8}	2.6626×10^{-7}	1.2173×10^{-5}	2.9430×10^{-7}
0.05	5.5280×10^{-10}	3.1597×10^{-7}	5.6723×10^{-10}	1.5428×10^{-8}	6.3028×10^{-7}	1.7453×10^{-9}
0.025	7.1619×10^{-11}	1.6134×10^{-8}	3.5361×10^{-11}	9.2885×10^{-10}	3.5562×10^{-8}	1.0862×10^{-10}
h		$r = 2$, linear splines				
		E_{amp}		E_{phase}		E_{shape}
0.1		4.0487×10^{-5}		1.7600×10^{-3}		6.7965×10^{-5}
0.05		2.7453×10^{-6}		3.3000×10^{-3}		1.6249×10^{-5}
0.025		2.2631×10^{-7}		9.5238×10^{-4}		4.0635×10^{-6}

Table 5 E_{amp}, E_{phase}, E_{shape} at $T = 100$, modified Galerkin method, peakon, $V = 1.333$

h	$r = 4$, cubic splines			$r = 3$, quadratic splines		
	E_{amp}	E_{phase}	E_{shape}	E_{amp}	E_{phase}	E_{shape}
0.05	1.1717×10^{-2}	6.4696×10^{-1}	2.5744×10^{-2}	1.6177×10^{-2}	1.0482×10^{0}	1.1215×10^{-2}
0.025	6.1999×10^{-3}	3.2055×10^{-1}	1.3246×10^{-2}	8.1867×10^{-3}	5.1723×10^{-1}	6.6000×10^{-3}
0.01	2.6237×10^{-3}	1.2855×10^{-1}	5.9284×10^{-3}	3.4618×10^{-3}	2.0548×10^{-1}	3.2406×10^{-3}
h		$r = 2$, linear splines				
		E_{amp}		E_{phase}		E_{shape}
0.05		1.1487×10^{-2}		6.5000×10^{-1}		5.8839×10^{-2}
0.025		7.1264×10^{-3}		3.0000×10^{-1}		3.2941×10^{-2}
0.01		3.5565×10^{-3}		1.1000×10^{-1}		1.3585×10^{-2}

The errors of the standard Galerkin method (for $r = 4$ and $r = 3$) were roughly the same. The errors did not oscillate in time and practically remained constant for the smaller values of h. Because the maximum of the peakon for linear splines coincides with the mesh node $x = 33.3$ at $T = 100$ the actual E_{phase} happened to be 0. For this reason we present the mean value of the E_{phase} for all times $t^n \in [80, 100]$. In all cases the speed was conserved to two digits when $h = 0.05$ and $h = 0.025$, and to three digits when $h = 0.01$.

5.5 Approximation of the generation and interactions of peakons

In closing we record some observations concerning the approximation of peakons by the fully discrete Galerkin methods under consideration:

(i) When a nonsmooth function such as a peakon is used as initial value in an evolution numerical experiment one expects a practically localized oscillatory error to appear at $t = 0$ as a result of projecting the peakon onto the finite element space. As previously mentioned we normally use as initial value of the discrete schemes the H^1 projection of the initial data; using the L^2 projection or the interpolant leads to similar errors.

As an example, consider the evolution shown in Fig. 4, in which a peakon of unit speed, initially centered at $x = 0$, is approximated by the H^1 projection in the space of quadratic splines and its evolution is effected by the fully discrete modified Galerkin method up to $T = 50$. An oscillatory error, decaying fast in space, of amplitude 7.5×10^{-3} for $h = 0.05$, is generated near $x = 0$ where the initial peakon was located. It diminishes slowly as h is decreased; for example its amplitude is about 1.6×10^{-3} when $h = 6.25 \times 10^{-3}$. A similar error is observed in the case of the standard Galerkin method for the other spline spaces; the modified method gives somewhat better results. We observed that the same type of error appears in spectral discretizations of the CH equation with the interpolant e.g. taken as initial condition.

This small noise remains stationary in time in the vicinity of the spatial point of its generation. Apparently this property is shared by the CH equation (due to the presence of the $-u_{xxt}$ term) with the BBM equation, for which, it was shown in [3] that initial discontinuities in the data do not propagate. (Similar errors, noticed in numerical solutions of the BBM equation in [5], were caused by the truncation of the decaying ends of an initial solitary-wave profile in that reference.)

(ii) Peakons, being solitons, interact elastically, and their overtaking collisions have been described in detail analytically cf. e.g. [15,39]. However, when their interactions are simulated by a numerical evolution method one observes that numerical artifacts, in the form of small residual waves, are produced.

As an example, we consider two peakons of amplitudes 1.0 and 0.5 centered initially at $x = -20$ and 20, respectively. With those initial values we integrate the RCH with periodic conditions on the interval $[-100, 100]$ using the fully discrete modified Galerkin method with cubic splines with $h = 5 \times 10^{-3}$ and $\Delta t = h/10$. The results of the numerical evolution up to $t = 200$ are shown in Fig. 5.

In Fig. 5c, at $t = 25$, we observe again the small oscillations (stationary in the vicinity of $x = -20$ and $x = 20$) produced by the H^1 projection of the initial

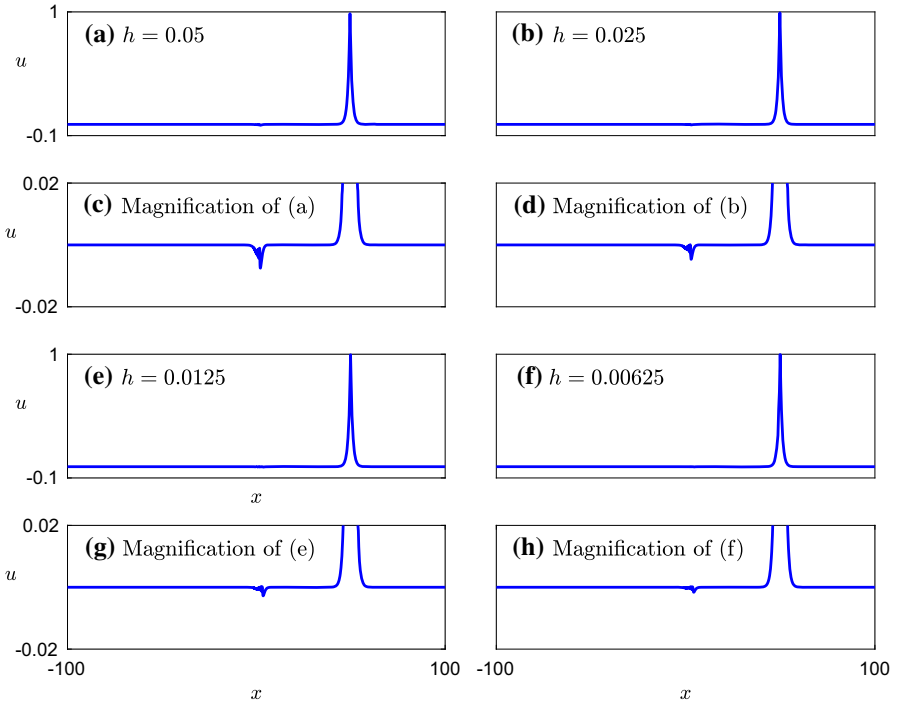

Fig. 4 Peakon propagation with the modified Galerkin method and quadratic splines for various values of h, $\Delta t = h/10$, $T = 50$

peakons in the finite element space and previously commented on. The peakons first interact in a spatial and temporal window centered at $(x, t) = (60, 80)$ and wrap around the boundary due to periodicity. At $t = 200$ (Fig. 5e, f) we observe the high frequency stationary oscillations produced near $x = 20$ due to the initial approximation of the smaller peakon. (The analogous oscillations produced near $x = -20$ by the projection of the larger peakon have 'climbed' on the larger peakon which is centered at $x = -20$ at this time instant.) We also observe near $x = 60$ a large-wavelength *wavelet* of amplitude about 2.8×10^{-4}. This wavelet is stationary; note that the dispersion relation of the linearized RCH is $\omega = 0$, and therefore small-amplitude disturbances are not expected to propagate. The wavelet is a numerical artifact produced by the numerical approximation of the peakon collision. Its amplitude diminishes slowly as h is decreased; e.g. it was equal to 5×10^{-4} when $h = 0.01$. The wavelet reappeared near $x = 60$ after the next interaction (due to periodicity), of the peakons, that occurred around $t = 480$. (In order to observe the wavelet after the subsequent interactions, which all occur near $x = 60$, one has to 'clean' smoothly the solution profile well after the first interaction from small-amplitude artifacts and let the main pulses interact again). That the wavelet is specific to the numerical interaction of peakons may also be seen from the fact that it is absent when overtaking collisions of *smooth* travelling waves of the RCH are simulated numerically. When we did so (with the same numerical method taking $h = 0.1$ and $\Delta t = h/10$), we observed that only the expected numerical

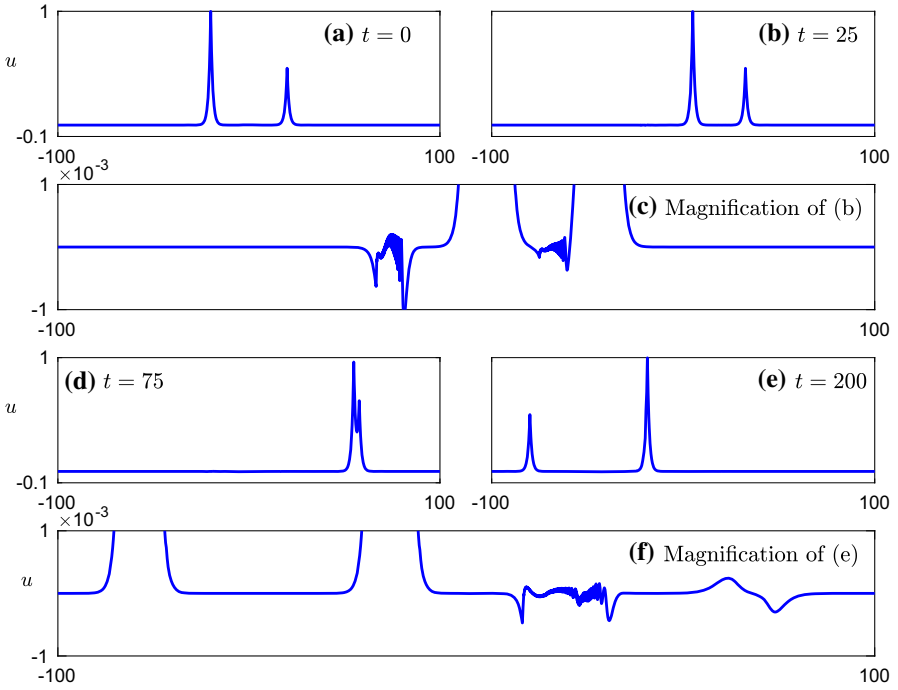

Fig. 5 Interaction of two peakons, modified Galerkin, cubic splines, $h = 0.005$, $\Delta t = h/10$

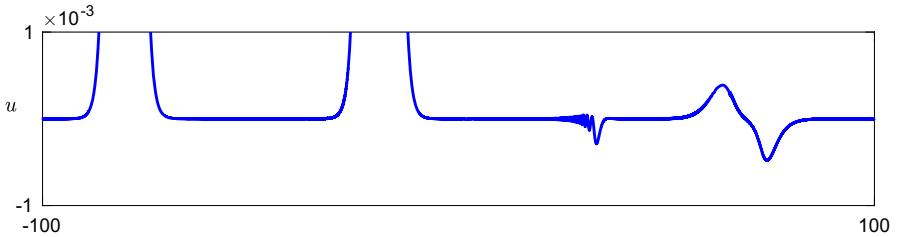

Fig. 6 Interaction of two peakons (evolution of Fig. 5) using the standard pseudospectral-RK4 method, $N = 16384$, $\Delta = 5 \times 10^{-3}$

dispersive tail was observed; the latter had an amplitude of $O(10^{-6})$ and diminished fast as h was decreased.

The wavelet also appears after numerical peakon interactions effected by other type of discretizations. For example, the pseudospectral-RK4 method with $N = 16,384$, $\Delta t = 5 \times 10^{-3}$ gives for the analogous experiment shown in Fig. 5, at $t = 200$ the profile given in Fig. 6, very similar to the one of Fig. 5f. The wavelet and the initial oscillations diminish slowly as N is increased and Δt is decreased. The fact that the numerical interaction of peakons with spectral methods give small errors that diminish slowly as the mesh is refined was already observed in [29]. Here we have pointed out that the small errors are of the two kinds depicted in Figs. 5 and 6.

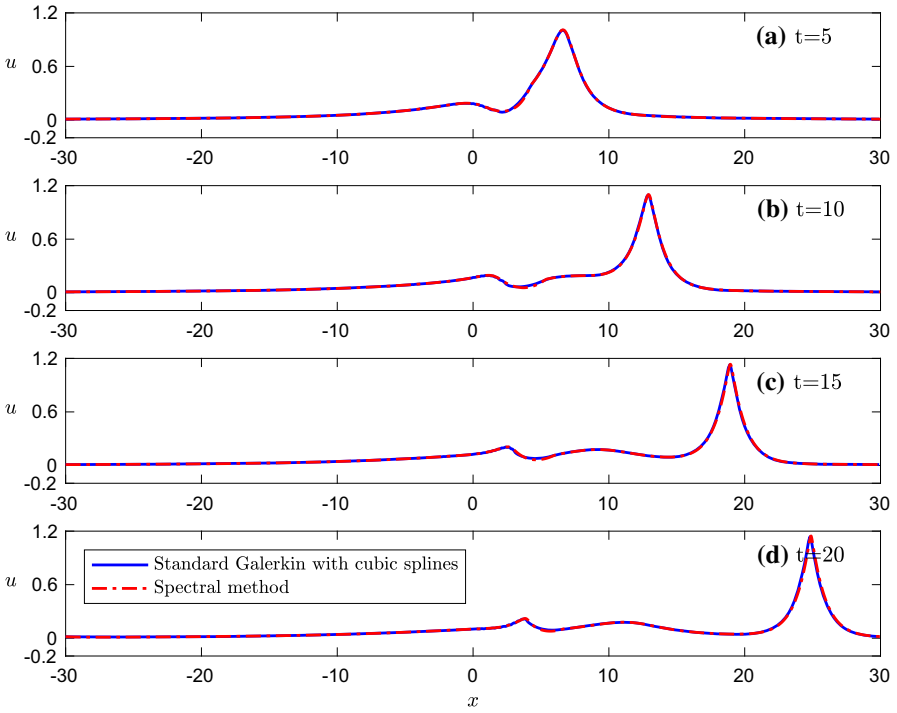

Fig. 7 Evolution of RCH with initial profile (5.10), standard Galerkin method with cubic splines and pseudospectral-RK4 scheme

(iii) We finally present results obtained by applying our numerical methods to two evolution problems for RCH that have been proposed in the literature as examples of peakon generation from continuous initial profiles that have discontinuous derivatives. The first, [10,25,41], corresponds to the initial value

$$u_0(x) = \frac{10}{(3+|x|)^2}, \quad x \in [-30, 30], \tag{5.10}$$

which we integrated up to $t = 20$ by our fully discrete standard Galerkin method with cubic splines using $h = 0.1$, $\Delta t = 0.001$, cf. Fig. 7. Superimposed on the spline graphs of Fig. 7 are the corresponding obtained by the usual pseudospectral-RK4 discretization of RCH with $N = 4096$, $\Delta t = 0.01$. (For smaller values of N the pseudospectral method had a noticeable phase error by $t = 20$.)

The second initial profile, [2,41], corresponds to the plateau function given by

$$u_0(x) = \begin{cases} c\, e^{x+5}, & x \le -5 \\ c, & |x| \le 5 \\ c\, e^{-x+5}, & x \ge 5 \end{cases} \quad x \in [-40, 40], \quad c = 0.6, \tag{5.11}$$

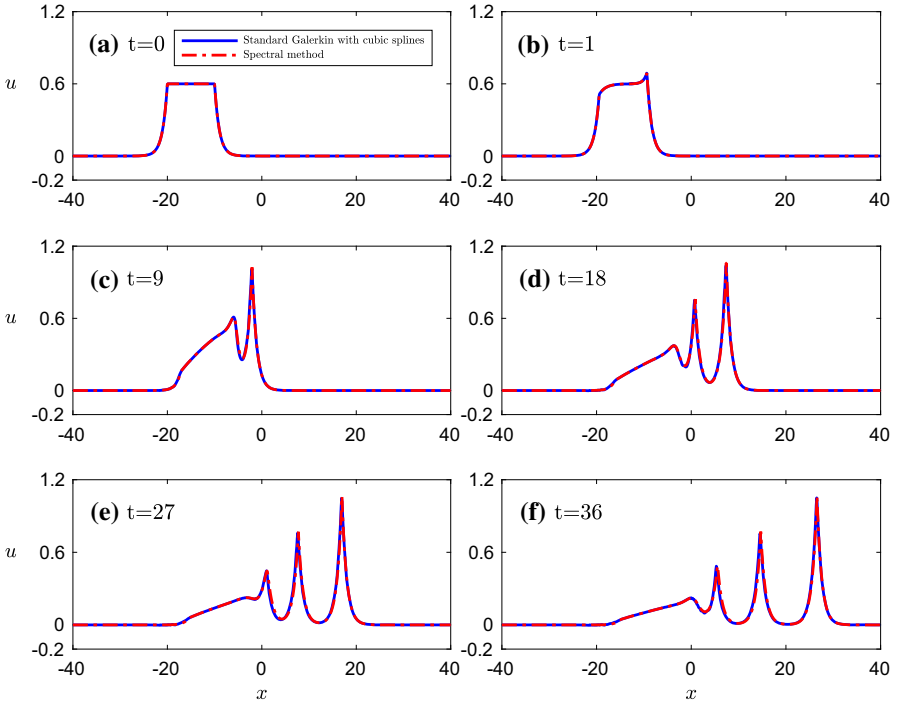

Fig. 8 Evolution of RCH with initial profile (5.11), Standard Galerkin method with cubic splines and pseudospectral-RK4

and produces the evolution shown up to $t = 36$ in Fig. 8. For the fully discrete standard Galerkin scheme with cubic splines we took $h = 0.1$ and $\Delta t = 0.01$. Superimposed are shown the corresponding profiles generated by the usual pseudospectral-RK4 scheme for $N = 8192$, $\Delta t = 0.001$. For smaller values of N the scheme exhibited phase and amplitude errors in approximating the larger emerging peakon. In both test problems the Galerkin method gave very accurate results.

Acknowledgements V.A.D. and D.E.M. acknowledge travel support by grant MTM2014-54710 of the Ministerió de Economia y Competividad, Spain. D.E.M. was supported by the Marsden Fund administered by the Royal Society of New Zealand with Contract Number VUW1418.

References

1. Antonopoulos, D.C., Dougalis, V.A., Mitsotakis, D.: On error estimates for Galerkin finite element methods for the Camassa–Holm equation (2018). arXiv:1805.10744
2. Artebrant, R., Schroll, H.J.: Numerical simulation of Camassa–Holm peakons by adaptive upwinding. Appl. Numer. Math. **56**, 695–711 (2006)
3. Benjamin, T.B., Bona, J.L., Mahony, J.J.: Model equations for long waves in nonlinear dispersive systems. Philos. Trans. R. Soc. Lond. A **272**, 47–78 (1972)

4. Bona, J.L., Dougalis, V.A., Karakashian, O.A., McKinney, W.R.: Conservative, high-order numerical schemes for the generalized Korteweg–de Vries equation. Philos. Trans. R. Soc. Lond. A **351**, 107–164 (1995)
5. Bona, J.L., Pritchard, W.G., Scott, L.R.: Numerical schemes for a model for nonlinear dispersive waves. J. Comput. Phys. **60**, 167–186 (1985)
6. Bressan, A., Constantin, A.: Global conservative solutions of the Camassa–Holm equation. Arch. Ration. Mech. Anal. **183**, 215–239 (2007)
7. Camassa, R., Holm, D.D.: An integrable shallow water equation with peaked solitons. Phys. Rev. Lett. **71**, 1661–1664 (1993)
8. Camassa, R., Holm, D.D., Hyman, J.M.: A new integrable shallow water equation. Adv. Appl. Mech. **31**, 1–33 (1994)
9. Chertock, A., Liu, J.-G., Pendleton, T.: Convergence of a particle method and global weak solutions of a family of evolutionary PDEs. SIAM J. Numer. Anal. **50**, 1–21 (2012)
10. Chertock, A., Liu, J.-G., Pendleton, T.: Elastic collisions among peakon solutions for the Camassa–Holm equation. Appl. Numer. Math. **93**, 30–46 (2015)
11. Coclite, G.M., Karlsen, K.H., Risebro, N.H.: A convergent finite difference scheme for the Camassa–Holm equation with general H^1 initial data. SIAM J. Numer. Anal. **46**, 1554–1579 (2008)
12. Constanin, A., Lenells, J.: On the inverse scattering approach to the Camassa–Holm equation. J. Nonlinear Math. Phys. **10**, 252–255 (2003)
13. Constantin, A.: On the Cauchy problem for the periodic Camassa–Holm equation. J. Differ. Equ. **141**, 218–235 (1997)
14. Constantin, A.: On the scattering problem for the Camassa–Holm equation. Proc. R. Soc. Lond. A **457**, 953–970 (2001)
15. Constantin, A., Escher, J.: Global existence and blow-up for a shallow water equation. Ann. Sc. Norm. Super. Pisa **26**, 303–328 (1998)
16. Constantin, A., Escher, J.: Wave breaking for nonlinear nonlocal shallow water equations. Acta Math. **181**, 229–243 (1998)
17. Constantin, A., Lannes, D.: The hydrodynamical relevance of the Camassa–Holm and Degasperis–Procesi equations. Arch. Ration. Mech. Anal. **192**, 165–186 (2009)
18. Constantin, A., Molinet, L.: Orbital stability of solitary waves for a shallow water equation. Physica D **57**, 75–89 (2001)
19. Constantin, A., Strauss, W.: Stability of peakons. Commun. Pure Appl. Math. **53**, 603–610 (2000)
20. Constantin, A., Strauss, W.: Stability of the Camassa–Holm solitons. J. Nonlinear Sci. **12**, 415–422 (2002)
21. Escher, J., Yin, Z.: Initial boundary value problems of the Camassa–Holm equation. Commun. Partial Differ. Equ. **33**, 377–395 (2008)
22. Fokas, A.S.: On a class of physically important integrable equations. Physica D **87**, 145–150 (1995)
23. Fuchssteiner, B.: Some tricks from the symmetry-toolbox for nonlinear equations: generalizations of the Camassa–Holm equation. Physica D **95**, 229–243 (1996)
24. Fuchssteiner, B., Fokas, A.S.: Symplectic structures, their Bäcklund tranformations and hereditary symmetries. Physica D **4**, 47–66 (1981)
25. Holden, H., Raynaud, X.: A convergent numerical scheme for the Camassa–Holm equation based on multipeakons. Discrete Contin. Dyn. Syst. **14**, 505–523 (2006)
26. Holden, H., Raynaud, X.: Convergence of a finite difference scheme for the Camassa–Holm equation. SIAM J. Numer. Anal. **44**, 1655–1680 (2006)
27. Johnson, R.S.: Camassa–Holm, Korteweg–de Vries and related models for water waves. J. Fluid Mech. **455**, 63–82 (2002)
28. Johnson, R.S.: On solutions of the Camassa–Holm equation. Proc. R. Soc. Lond. A **459**, 1687–1708 (2003)
29. Kalisch, H., Lenells, J.: Numerical study of traveling-wave solutions for the Camassa–Holm equation. Chaos Solitons Fractals **25**, 287–298 (2005)
30. Kalisch, H., Raynaud, X.: Convergence of a spectral projection of the Camassa–Holm equation. Numer. Methods Partial Differ. Equ. **22**, 1197–1215 (2006)
31. Kwek, K.H., Gao, H., Zhang, W., Qu, C.: An initial boundary value problem of Camassa–Holm equation. J. Math. Phys. **41**, 8279–8285 (2000)
32. Lenells, J.: Traveling wave solutions of the Camassa–Holm equation. J. Differ. Equ. **217**, 393–430 (2005)

33. Li, Y.A., Olver, P.J.: Well-posedness and blow-up solutions for an integrable nonlinearly dispersive model wave equation. J. Differ. Equ. **162**, 27–63 (2000)
34. Liu, H., Xing, Y.: An invariant preserving discontinuous Galerkin method for the Camassa–Holm Equation. SIAM J. Sci. Comput. **38**, A1919–A1934 (2016)
35. Molinet, L.: On well-posedness results for Camassa–Holm equation on the line: a survey. J. Nonlinear Math. Phys. **11**, 521–533 (2004)
36. Parker, A.: On the Camassa–Holm equation and a direct method of solution I. Bilinear form and solitary waves. Proc. R. Soc. Lond. A **460**, 2929–2957 (2004)
37. Parker, A.: On the Camassa–Holm equation and a direct method of solution. II. Soliton solutions. Proc. R. Soc. Lond. A **461**, 3611–3632 (2005)
38. Parker, A.: On the Camassa–Holm equation and a direct method of solution. III. N-soliton solutions. Proc. R. Soc. Lond. A **461**, 3893–3911 (2005)
39. Parker, A.: Wave dynamics for peaked solitons of the Camassa–Holm equation. Chaos Solitons Fractals **35**, 220–237 (2008)
40. Thomée, V., Wendroff, B.: Convergence estimates for Galerkin methods for variable coefficient initial value problems. SIAM J. Numer. Anal. **11**, 1059–1068 (1974)
41. Xu, Y., Shu, C.-W.: A local discontinuous Galerkin method for the Camassa–Holm equation. SIAM J. Numer. Anal. **46**, 1998–2021 (2008)